Evidence for seven-fold cobalt coordination at the $CoSi_2$/Si(111) interface

1989 J. Phys.: Condens. Matter 1 3999

(http://iopscience.iop.org/0953-8984/1/25/011)

J. Phys.: Condens. Matter 1 (1989) 3999–4004. Printed in the UK

LETTER TO THE EDITOR

Evidence for seven-fold cobalt coordination at the $CoSi_2/Si\langle 111\rangle$ interface

A Catana†, P E Schmid†, S Rieubland†, F Lévy† and P Stadelmann‡

† Institute of Applied Physics, Swiss Federal Institute of Technology, 1015 Lausanne, Switzerland

‡ Institute of Electron Microscopy, Swiss Federal Institute of Technology, 1015 Lausanne, Switzerland

Received 31 March 1989

Abstract. $CoSi_2/Si\langle 111\rangle$ interfaces have been prepared by annealing of a UHV-evaporated, Co layer at 500, 600, and 900 °C. Using electron microscopy at atomic-scale resolution, we have compared experimental pictures with an extensive set of calculated images. Our observations support Si–Si interfacial bonds consistent with a seven-fold coordination of the first Co layer. This is the first evidence of this interface geometry for $CoSi_2$, other reports being in favour of Co–Si bonds and a five-fold or eight-fold Co coordination.

Epitaxial silicide/silicon interfaces and especially the $CoSi_2/Si$ system have recently motivated a large number of studies. The key points are related, with both technological and fundamental aspects. In particular, the bonding at the $CoSi_2/Si\langle 111\rangle$ interface is a current subject of both experimental (Rossi *et al* 1989, Fischer *et al* 1987, 1988, Wu *et al* 1986, d'Anterroches *et al* 1986) and theoretical (Hamann 1988, van den Hoek *et al* 1988) investigations. In this Letter, we report on the interface composition and bonding configuration at the $CoSi_2/Si$ interface by comparing high-resolution electron microscopy (HREM) images with model calculations. Previously, evidence for the five-fold interface model was reported by Gibson *et al* (1982) and for the eight-fold model by Rossi *et al* (1989). We report the first observation of the seven-fold model. This configuration is the same as the one described by Cherns *et al* (1982) for $NiSi_2/Si$. Theoretical calculations (Hamann 1988) of the interfacial energy indicate that the seven-fold model is the most favourable for $NiSi_2/Si$ and is a close second for $CoSi_2/Si$.

$\langle 111\rangle$-oriented Si substrates were first cleaned by heating at 950 °C in a UHV chamber with a base pressure of 2×10^{-8} Pa. Subsequently, Co layers were deposited by a differentially pumped e-gun at a rate of 0.2 nm min^{-1}. During evaporation, the pressure increased to less than 9×10^{-8} Pa. The chemical composition and contaminants were checked by Auger spectroscopy. The samples were then annealed by Joule heating of the substrate to 500, 600 and 900 °C for a few minutes. The thickness of the silicide layer ranged from 3 to 12 nm. About 20 thin samples cut from each substrate were prepared for cross-sectional TEM investigations using conventional ion-thinning techniques. The HREM observations were performed on a Phillips 430ST microscope with a point resolution better than 0.2 nm.

0953-8984/89/253999 + 06 $02.50

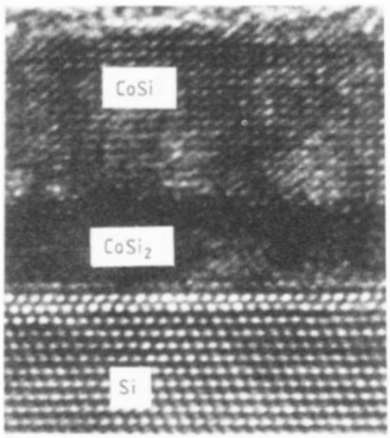

Figure 1. Cross-sectional view of CoSi layer on top of a B-type $CoSi_2$/Si(111) interface. The sample was processed at 500 °C.

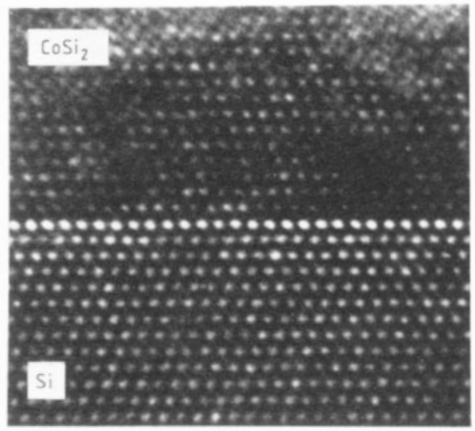

Figure 2. HREM micrograph of a typical B-type $CoSi_2$/Si interface region after a 900 °C anneal. Atomic positions are imaged in black.

The low lattice-constant mismatch is responsible for the good epitaxial growth of $CoSi_2$ on Si. The experimental results show flat and abrupt interfaces. The low-temperature treatment results in the formation of both A- and B-type $CoSi_2$/Si regions. Moreover, the sample annealed at 500 °C shows regions of epitaxial CoSi on top of $CoSi_2$, indicating an incomplete reaction. This result suggests that the formation of $CoSi_2$ takes place predominantly at the CoSi/Si interface rather than at the CoSi/vacuum interface. The orientation relationship between CoSi and $CoSi_2$ is expressed by: $[1\bar{1}2]CoSi \parallel [110]CoSi_2$, $(1\bar{1}\bar{1})CoSi \parallel (1\bar{1}\bar{1})CoSi_2$. This corresponds to a 30° rotation around $[1\bar{1}\bar{1}]$ and represents a position of best fit between both crystal lattices. At higher temperatures, CoSi transforms to $CoSi_2$ and the B-type interface geometry dominates. After a 900 °C anneal, no A-type $CoSi_2$/Si region could be observed. Typical high-resolution micrographs of samples annealed at 500 and 900 °C are displayed in figures 1 and 2.

We consider now four interface bonding models that differ in the coordination of the Co atoms at the interface. The bulk $CoSi_2$ crystal has a CaF_2 structure in which the Co atoms are eight-fold coordinated. The five-fold coordination interface model corresponds to the situation where the terminal Co atoms at the interface have five Si neighbours only. The interface is represented in this case by Co–Si bonds. In the seven-fold model interfacial Co loses one Si neighbour with respect to its bulk coordination and the interface is characterised by Si–Si bonds. A first eight-fold coordination model assumes that the metal atoms at the interface have the same nearest neighbours as in bulk $CoSi_2$. This is possible if a Si layer, with one unsatisfied bond per atom, is added in the five-fold model. For this reason, we call this interfacial arrangement the eight-fold (5) model. Theoretical calculations conclude that this model has the lowest interface energy. Starting from the seven-fold geometry, the eight-fold coordination of Co at the interface can also be obtained by the introduction of either a Si layer with three unsatisfied bonds per atom (which seems rather unlikely) or a Co layer with one unsatisfied bond per atom. This configuration will be referred to as eight-fold (7). The geometric and compositional differences between the interface models are illustrated in figure 3.

After conventional processing of the samples, high resolution micrographs were taken at different defocus settings along the [110] direction. An indication about the

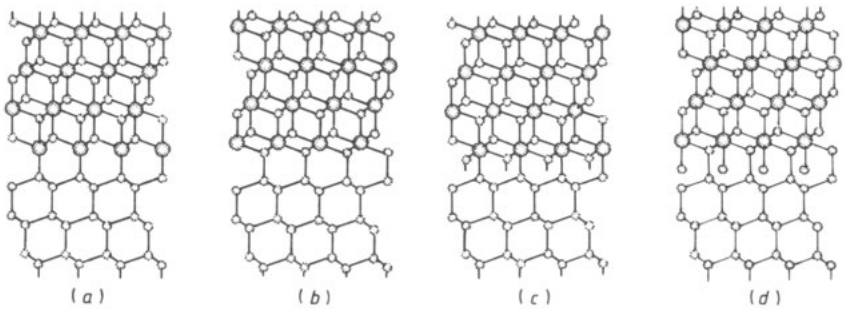

Figure 3. Interface models considered for B-type $CoSi_2$/Si. (*a*) five-fold, (*b*) seven-fold, (*c*) eight-fold (5) and (*d*) eight-fold (7).

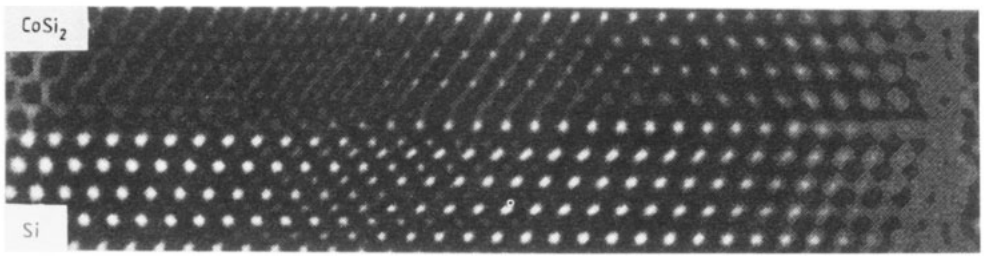

Figure 4. Image computation of a 98° wedge-shaped crystal showing thickness-induced contrast changes for a 48 nm defocus. The thickness varies linear from 0 nm (right edge) to 25 nm.

defocus is obtained after consideration of optical diffractograms of amorphous material near the specimen edge. However, for a precise determination of this parameter, image calculations were performed for increasing defocus values. The calculations were compared with images recorded at different calibrated defocus steps of the microscope. The image calculations were carried out using a multi-slice algorithm developed by one of us (Stadelmann 1987). The supercell slice used for the calculation is 5.61 nm along, 0.61 nm wide and 0.38 nm thick. It consists of 88 atoms and the sampling is 512 × 64, which is sufficient for an accurate representation of the atomic positions. Specimen thickness is another important parameter that determines the contrast of the HR image. In order to investigate the thickness variations which could be introduced during sample preparation, a careful calibration must be carried out prior to any image interpretation. A first approach comprises the observation of Fresnel fringes as one moves away from the edge of the specimen. Since no contrast reversal is observed, the thickness is certainly less than 10 nm.

For a more accurate thickness calibration, multi-slice calculations of wedge-shaped samples were carried out and compared with experimental images. This method is useful in producing images over a continuous thickness range and gives information about thickness-related contrast variations in both crystals simultaneously. Such a calculation is displayed in figure 4 for a 48 nm defocus. Comparison with experimental images shows that the thickness in the observed regions ranges from 3 to 7 nm. Figures 5 and 6 show comparisons between HR and calculated images for the interface-bonding models considered. On the left side of each simulation, dots mark the position of the atomic

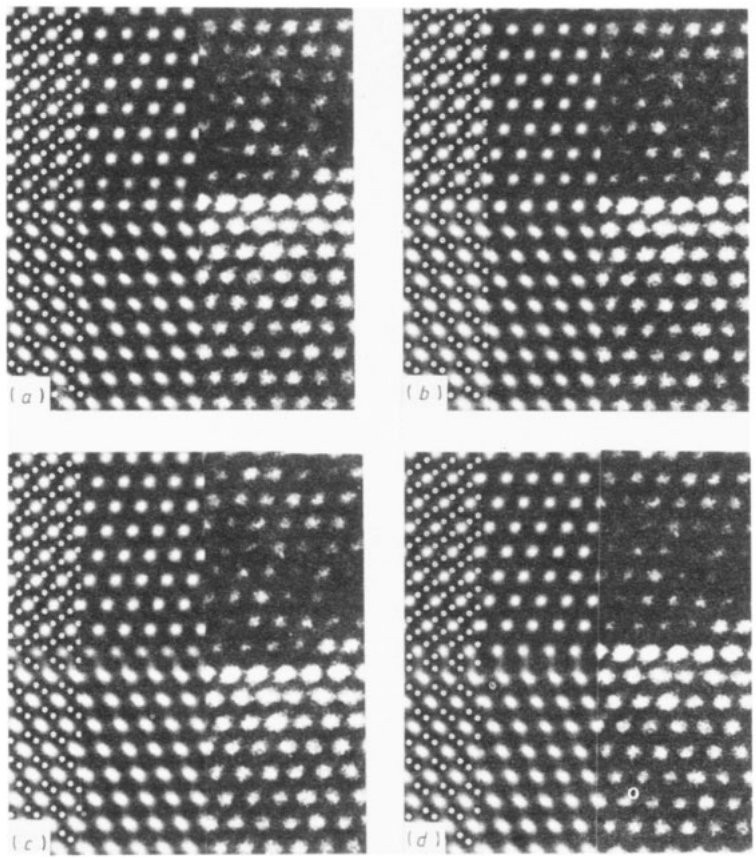

Figure 5. Simulated image of a 4 nm thick sample at 48 nm defocus (left) and experimental image (right). (*a*) five-fold, (*b*) seven-fold, (*c*) eight-fold (5) and (*d*) eight-fold (7).

columns. The microscope is characterised by the following parameters: spherical aberration coefficient = 1.1 mm, spread of focus = 10 nm and beam semiconvergence = 1 mrad. The simulations were carried out at two defocus values (48 nm and 99 nm) for a 4 nm thick sample. In the first case, black spots correspond to atomic columns. In the second case, the contrast is reversed, and the 0.19 nm fringes corresponding to the {220} planes are transmitted with a higher intensity. Under these conditions finer details of the interface structure are visible. The contrast variations induced by differences in atomic composition at the interface can be better resolved. These experimental images are typical of all our samples. A detailed analysis of the relative displacements between the atomic columns excludes the five-fold and eight-fold (5) models and designates the seven-fold model as being appropriate. This result is confirmed by the interface-contrast analysis. Moreover, one must also exclude the presence of an additional Si or Co layer at the interface that would saturate the metal atom coordination: the contrast changes would be clearly observable. The only interface model consistent with both experimental and simulated images is the seven-fold model. The A-type epitaxy was also observed, but only on samples annealed at low temperature. The results related to the A-type epitaxy will be discussed elsewhere.

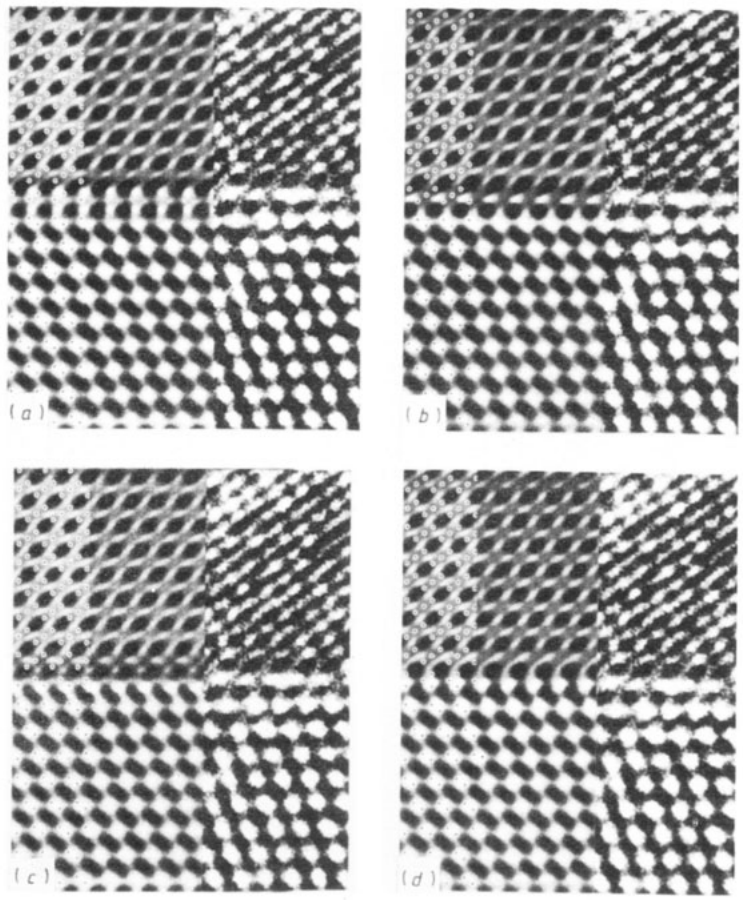

Figure 6. Simulated image of a 4 nm thick sample at 99 nm defocus (left) and experimental image (right). (*a*) five-fold, (*b*) seven-fold, (*c*) eight-fold (5) and (*d*) eight-fold (7).

Our analysis of the $CoSi_2$/Si system is based on observations at interfaces between massive slabs of $CoSi_2$ and Si. The eight-fold model has been shown to apply when $CoSi_2$ is separated from the vacuum by two Si layers only (Hellman *et al* 1988). A different interfacial configuration may also develop when only one or two $CoSi_2$ layers are buried into Si.

The interfacial energy difference between A-type and B-type epitaxies of $CoSi_2$ on Si is small and favours B-type orientation. Only B-type epitaxy is observed after a high temperature anneal. Clearly, a path exists that allows this system to minimise its interface energy with respect to A and B orientations. Theoretical calculations predict that indeed type B interface is slightly more favoured than type A. A larger energy difference is expected in relation to seven-fold and eight-fold interface geometries. One may suspect, then, that in the particular case of $CoSi_2$, an energy barrier is preventing the system from reaching its interfacial energy minimum.

In summary, the $CoSi_2$/Si⟨111⟩ interface was investigated using HREM along [110]. After low-temperature annealing (500 °C) an epitaxial CoSi layer is observed on top of $CoSi_2$, indicating an incomplete reaction. Various bonding models for the B-type $CoSi_2$/Si interface are discussed. The matching between corresponding calculated images and

experimental observations shows that the interface is characterised by a seven-fold coordination of the first Co layer. The relative rigid-body displacement is such that the Si atoms in the top layer of the Si⟨111⟩ substrate bond to the Si atoms in the silicide. Moreover, contrast analysis in the interface region excludes the presence of any extra interfacial layer which would thus increase the coordination of the terminal metal atom.

We wish to thank M Heintze for helpful discussions in the course of this work.

References

Cherns D, Anstis G R and Hutchison J L 1982 *Phil. Mag.* A **46** 849
D'Anterroches C and d'Avitaya F A 1986 *Thin Solid Films* **13** 351
Fisher A E M J, Gustafsson T and Van der Veen J F 1988 *Phys. Rev.* B **37** 6305
Fisher A E M J, Vlieg E, Van der Veen J F, Clausnitzer M and Materlik G 1987 *Phys. Rev.* B **36** 4769
Gibson J M, Bean J C, Poate J M and Tung R T 1982 *Appl. Phys. Lett.* **41** 818
Hamann D R 1988 *Phys. Rev. Lett.* **60** 313
Hellman F and Tung R T 1988 *Phys. Rev.* B **37** 10786
Rossi G, Jiu X, Santanielo A, DePadova P and Chandesris D 1989 *Phys. Rev. Lett.* **62** 191
Stadelmann P 1987 *Ultramicroscopy* **21** 131
van den Hoek P J, Ravenek W and Baerends E J 1988 *Phys. Rev. Lett.* **60** 1743
Wu S C, Wang Z Q, Li Y S, Jona F and Marcus P M 1986 *Phys. Rev.* B **33** 2900